DRYING AND DEVOLATILIZATION OF MISSISSIPPI LIGNITE IN A FLUIDIZED BED

Pradeep K. Agarwal, William E. Genetti, Yam Y. Lee

Chemical Engineering Department
University of Mississippi, University, MS 38677

INTRODUCTION

Fluidized bed combustion offers a means of burning coal and other low grade fuels with high moisture and ash content in an economical and environmentally acceptable way. Fluidized bed combustors can be made to reduce SO_2 and NO_x emission by suitable control of the combustion process eliminating the need for flue gas treatment (1,2).

Low rank coals such as Mississippi lignite contain appreciable amounts of moisture in their "as-mined" state. Hence, lignite particles being introduced into the combustor will undergo several processes before they are completely burned. These processes include, drying (with or without shrinkage), devolatilization, and combustion of volatiles and residual char. All these processes are expected to occur in overlapping time periods and their interactions are not well understood (3).

In this paper, a model is presented which describes the coupled drying and devolatilization of low rank coals in fluidized beds. Experiments are also performed in a three inch ID fluidized bed unit using alumina as bed particles to obtain data for drying and devolatilization of Mississippi lignite. The model predictions are then compared with the experimental data obtained.

BACKGROUND

The complexity of the drying process has led to large disparity between science and application (4). Based on the various mechanisms proposed for the movement of moisture in porous media, and at different levels of complexity and detail, several models have been reported. Dayan (5), however, points out that most of the models proposed may not be valid for intense drying conditions.

In fluidized beds operating at high temperatures, the drying process involves finite sized particles and finite drying times. Hence, semi-infinite strip formulations and asymptotic time domain solutions may not be valid. Moreover, using the reported correlations for gas solid heat exchange within fluidized beds and the thermophysical properties of coal, it may be shown that the heat transfer Biot numbers - for particle sizes and operating conditions of interest in FBC - may also vary within the range of 1 to 20 (6). This implies that instantaneous surface heat-up boundary conditions may also not be valid.

Rigorous and approximate methods for analyses of heat transfer problems with moving boundaries have been reviewed by Mori and Araki (7). Several numerical schemes have been proposed (8). However, numerical solutions have been found to be time consuming and difficult to implement. Additionally convective boundary conditions (of the second kind), which could reasonably describe the intense fluidized bed drying, have been noted to give rise to special difficulties both numerically as well as analytically (9,10).

Extensive reviews dealing with pyrolysis of predried coals are available in literature (11, 12, 13). The majority of the studies have focused on the determination of the kinetic mechanism and parameters using pulverized coal. It is becoming increasingly accepted that the overall coal decomposition kinetics cannot be represented by simple n^{th} order kinetic expressions because of two major reasons. The first is their inability to account for the observed final temperatue dependent yields and the second is the lower activation energies and preexponential factors for the Arrhenius rate expressions (11,12).

Large particle coal decomposition studies, which would involve consideration of the decomposition kinetics as well as transport processes, are comparatively few. Mechanisms proposed include heat (14, 15, 16) as well as mass transfer controlled devolatilization rates (17,18). Available experimental evidence for devolatilization in inert atmospheres suggests that the total devolatilization time would be proportional to d^2, where d is the particle diameter. However, since the transient transport of heat as well as mass is represented in terms of $Fo = \alpha t/d^2$, the experimental evidence does not directly distinguish between heat and mass transfer control.

THE MODEL

The proposed model for coupled drying and devolatilization of coal is based on the models proposed earlier for drying (6) and devolatilization of predried coal (19).

The moisture and volatile species are assumed to be evenly distributed within the spherical particle of radius R_o. The particle is assumed to retain its shape during the process. Devolatilization is assumed to be thermally neutral. Mass transfer is assumed to be rapid. Heat transfer – to and through the particle – is assumed to be the rate controlling mechanism for drying which is assumed to take place from a receding drying (phase change) front constituting a moving boundary. Heat transfer in conjunction with the overall coal decomposition kinetics is assumed to be the rate controlling step for devolatilization.

From the time the wet coal particle is introduced into the fluidized bed, there would be two different stages which are analyzed separately in the following:

Stage 1

When the wet coal particle is introduced into the fluidized bed, drying would commence almost immediately with the moving boundary constituting the drying front moving inwards. The heat conduction equation, with a constant effective thermal diffusivity, may be written for the dry shell region as

$$\frac{\partial T}{\partial t} = \frac{\alpha}{r^2} \frac{\partial}{\partial r} (r^2 \frac{\partial T}{\partial r}) \qquad r_e \leq r \leq R_o \qquad 1)$$

The convective boundary condition (of the second kind) at the particle surface is

$$\left. k_s \frac{dT}{dr} \right|_{r = R_o} = h (T_a - T_s) \qquad \text{for finite h and } T_s \neq T_a \left.\begin{array}{c} \\ \\ \\ \\ \end{array}\right\} \quad 2)$$
$$= a(t) \qquad \text{in general}$$

At the receding wet dry interface, a heat balance leads to

$$k_s \frac{dT}{dr}\bigg|_{r = r_e} = \lambda \ C_o \ \rho_s \frac{dr_e}{dt}$$ 3)

The moving boundary may be immobilized by a transformation of the space variable as $\phi = (r - r_e)/(R_o - r_e)$. The temperature profile, assumed to be quadratic with coefficients evaluated by the initial and boundary conditions, may be found to be

$$T(r,t) = T_e + (T_s - T_e)(2\phi - \phi^2) + a(t)((R_o - r_e)/k_s)(\phi^2 - \phi)$$ 4)

Use of the heat balance integral approach leads to an equation involving integrals which can be evaluated given the particle surface temperature as a function of time. The assumption that a pseudo steady state formulation (20) may be used to estimate the surface temperature then leads to the following governing equation to describe the drying

$$B\phi_m^3 + (D-E_1-B)\phi_m^2 + (C-B-D)\phi_m + B - C + E_1 - A.F = 0$$ 5)

where $\phi_m = \dfrac{r_e}{R_o}$ and the coefficients A, B, C, D, E_1 and F are tabulated in Table 1.

TABLE 1. Coefficients of the Governing Equation of Drying (Equation 5)

$A = (\dfrac{T_e + L}{2}) - \dfrac{T_e + 5 \ T_s\big|_{\theta=1}}{12} + \dfrac{Bi \ \phi_{ms}\big|_{\theta=1}}{12(2\phi_{ms}\big|_{\theta=1}} \dfrac{(T_a - T_e)}{+ Bi \ (1 - \phi_{ms}\big|_{\theta=1}))}$		
$B = \dfrac{\phi_{ms} \ Bi \ (T_a - T_e)}{12 \ (2\phi_{ms} + Bi \ (1 - \phi_{ms}))}$	$C = \dfrac{T_e + 5 \ T_s}{12}$	
$D = \dfrac{T_e + T_s}{4}$	$E_1 = (\dfrac{T_e + L}{2})$	$F = (\dfrac{\phi_{ms}^2 - 1}{\dfrac{\phi^2_{ms}\big|_{\theta=1}}{} - 1})$
$L = \dfrac{\lambda \ C_o}{C_p}$	$\lambda' = \lambda + (T_e - T_o)(C_{pw} + C_p/C_o)$	

The volumetric average fractional devolatilization is given by

$$X_c = \frac{3}{R_o^3} \int_o^{R_o} X \ r^2 \ dr$$ 6)

where X is the point devolatilization expression given by the non-isothermal kinetic expression proposed by Anthony et al. (11)

$$X = \int_{o}^{\infty} \exp(-k_o \int_o^t e^{-E/RT}) \ f(E) \ dE$$

$$f(E) = [\sigma(2\pi)^{\frac{1}{2}}]^{-1} \exp[-(E - E_o)^2/2\sigma^2]$$

7)

Recognizing that there would be no devolatilization in the wet region and that $_o\int^{\infty} f(E) \ dE = 1$, it may be shown

$$X_c = \frac{3}{R_o^3}\left[\frac{r_e^3}{3} + \int_{r_e}^{R_o} [\int_o^{\infty} \exp(-k_o \int_o^t e^{-E/RT} \ dt) \ f(E) \ dE] \ r^2 \ dr \right]$$

8)

Equation 8 may be integrated numerically with the temperature profile given by equation 4 to characterize devolatilization in the presence of simultaneous drying.

Stage 2

After the drying is completed, the particle would still devolatilize until the remaining possible devolatilization at the operating temperature is completed. Writing the heat conduction equation with time $t´ = t - \tau$, where τ is the time required for the completion of drying

$$\frac{\partial T}{\partial t´} = \frac{\alpha}{r^2} \frac{\partial}{\partial r} (r^2 \frac{\partial T}{\partial r}) \qquad\qquad 0 < r < R_o$$

9)

The boundary conditions for finite Biot numbers may be written as

$$k_s \frac{dT}{dr}\bigg|_{r = R_o} = h(T_a - T_s)$$

$$\frac{dT}{dr}\bigg|_{r = o} = 0$$

10)

The initial condition is derived from equation 4 with $r_e = 0$.   Then

$$T(r, t´ = 0) = T(r, t = \tau) =$$

$$T_e + (T_s\big|_{\theta=1} - T_e)(2 \ (\frac{r}{R_o})^2 - (\frac{r}{R_o})) + a(t)\big|_{\theta=1} (\frac{R_o}{k_s})((\frac{r}{R_o})^2 - \frac{r}{R_o})$$

11)

Following the analysis methods described by Jakob (21), it is possible to show that during this stage

$$T(r,t) = T_a - \sum_{i=1}^{\infty} N_i (\frac{\sin \beta_i \ r/R_o}{\beta_i \ r/R_o})e^{-\frac{\beta_i^2 \ t}{R_o^2}}$$

12a)

where β_i's are the roots of the equation

$$\beta \cos \beta = (1 - Bi) \sin \beta$$

12b)

and $N_i = 2 [C_1A_1 - (2C_2 - C_3)A_2 - (C_3 - C_2)A_3]/A_4$. The expressions for C_1, C_2, C_3. A_1, A_2, A_3 and A_4 are tabulated in Table 2.

TABLE 2. Coefficients Defining Equation 12

$A_1 = \sin \beta_i - \beta_i \cos \beta_i$		$A_2 = \cos \beta_i (\frac{2}{\beta_i} - \beta_i) + 2 \sin \beta_i - \frac{2}{\beta_i}$	
$A_3 = \cos \beta_i (\frac{6}{\beta_i} - \beta_i) + 3 \sin \beta_i (1 - \frac{2}{\beta_i^2})$		$A_4 = \beta_i - \sin \beta_i \cos \beta_i$	
$C_1 = (T_a - T_e)$	$C_2 = (T_s - T_e)$		$C_3 = a(t) \frac{R_o}{k_s}$

The temperature profile given by equation 12 may now be used in the expression for volumetric average fractional devolatilization to characterize the devolatilization in the second stage.

The flow chart of the computational procedure is shown in Figure 1.

EXPERIMENTAL APPARATUS

The fluidized bed used was 7.6 cm in diameter. The bed was filled to a static height of 12.7 cm with 6-10 mesh alumina beads. Preheated air/nitrogen, introduced into the bed through a perforated steel place distributor, was used to fluidize the bed. The air/nitrogen flow rate into the bed and the bed temperatures were measured by an orificemeter and thermocouples respectively. A schematic diagram of the experimental set up is given in Figure 2.

Large chunks of Mississippi lignite were broken and crushed to 4-7 mesh size. Samples were stored in polyethylene bags to prevent loss of moisture and shaken virorously to ensure a homogeneous mixture. Random samples were withdrawn and analyzed on Fischer Proximate Analyzer to determine initial moisture and volatile content (given in Table 3).

A cylindrical cage shaped sampler was constructed from woven mesh (10 mesh aperture size) of steel. The bottom of the sampler was fixed and the top was a removable cap. The sampler was provided with a handle to facilitate insertion into and withdrawal from the bed. The bed was brought up to the required temperature with air as the fluidizing medium. Nitrogen, however, was used during the actual experiment to prevent combustion. The empty sampler was inserted into the bed to permit it to reach the bed temperature. It was then withdrawn, a batch of lignite particles was put into the sampler and the cap closed. The sampler, with the lignite, was inserted within the bed for the desired time period and then withdrawn. The lignite particles were quenched, weighed and analyzed for the residual amount of moisture and volatiles in the Proximate Analyzer. Several readings were taken for each time period to ensure reproducibility.

RESULTS AND DISCUSSION

Experimental data for drying (6) for Mississippi lignite (for temperatures <200°C) and for devolatilization (22) of predried Mississippi lignite (for a different bed particle size and fluidizing velocity) have been reported earlier. The above are the limiting cases for the general model presented in this paper. Hence, the data presented earlier may be viewed in conjunction with the data presented here. The comparison of the data for the coupled process - for drying (O) with model calculations (—) and for devolatilization (☐) with model calculations (— - —) - are shown in Figures 3 and 4. The parameters used in the present model calculations are the same as used in the studies of the phenomena examined separately (6, 22) and are tabulated in Table 3.

<p align="center">Table 3.</p>

I. Experimental Operating Conditions:	

$u = 1.5$ m/s $\qquad C_O = 0.68$ gm/gm dry coal
Initial volatile content $= 0.5$ gm/gm dry coal
Coal Particle Sizes: 4-7 mesh (average $d = 3.8$ mm)
$T_a = 713°K \qquad - \quad Bi \simeq 3.0$
$T_a = 613°K \qquad - \quad Bi \simeq 4.0$

II. Kinetic and Thermophysical Properties (6,22)

$\alpha = 0.1$ mm^2/s $\qquad T_o = 283°K \qquad \lambda = 570$ cal/gm
$\rho_s = 1.25$ gm/cm^3 $\qquad T_e^o = 373°K \qquad C_p = 0.3$ cal/gm°K
$E_o = 192$ kJ/mol $\qquad \sigma = 40$ kJ/mol

The agreement of the model calculations with the data is seen to be good. The heat transfer approach, as presented here, is felt to be adequate at least for low rank coals (with low tar yields). A more accurate representation of the phenomena would require the use of the coupled heat and mass transfer solutions to describe the drying. Mass transport may also have to be included in describing the devolatilization of other types of coal with higher tar yields. However, it must be recognized that for FBC there is also the need to couple the phenomena of combustion of volatiles and the residual char. Thus, simplicity in model formulations is essential in order to make a complete analysis tractable. The strength of the model presented here is its ability to provide a reasonably rigorous and computationally tractable base to formulate an integrated approach for describing the various interactive processes occuring during the fluidized bed combustion of wet low rank coals.

NOMENCLATURE

A	coefficient, defined in Table 1
A_1	coefficient, defined in Table 2
A_2	coefficient, defined in Table 2
A_3	coefficient, defined in Table 2
A_4	coefficient, defined in Table 2
a	heat flux at the surface, watts/cm^2
B	coefficient, defined in Table 1
Bi	heat transfer Biot number, dimensionless
C	coefficient, defined in Table 1
C_1	coefficient, defined in Table 2

C_2	coefficient, defined in Table 2
C_3^2	coefficient, defined in Table 2
C_o	initial moisture content, gms moisture/gm dry coal
C^o	specific heat of coal, cal/gm°K
C^p	specific heat of water, cal/gm°K
D^{pw}	coefficient, defined in Table 1
d	particle diameter, mm
E_1	coefficient, defined in Table 1
E	activation energy, kJ mol^{-1}
E_o	mean activation energy, kJ mol^{-1}
F	coefficient, defined in Table 1
Fo	Fourier number, dimensionless
$f(E)$	Gaussian distribution function
h	heat transfer coefficient, cal/sec cm^2°K
k_o	pre-exponential factor in Arrhenius rate expression, sec^{-1}
k_s	thermal conductivity of coal, cal/cm sec°K
N_i	coefficients
R	gas constant, kJ/mol°K
R_o	particle radius, mm
r_e	radial position of the drying front, mm
r	radial position within a particle, mm
T	temperature, °K
T_a	ambient/bed temperature, °K
T_e	temperature at the drying front, °K
T_o	initial particle temperature, °K
t'	$t - \tau$, redefined time variable, sec
t	time, sec
X_c	fractional amount of volatiles retained
X	devolatilization at any point within the volume of the particle

Greek Letters

α	thermal diffusivity of coal, mm^2/sec
ϕ	$(r-r_e)/(R_o-r_e)$, transformed space variable
ϕ_m	r_e/R_o
τ	total drying time, sec
θ	t/τ, dimensionless time
ρ_s	particle density of the coal, gm/cm^3
λ	latent heat of vaporization of water, cal/gm
λ'	defined in Table 1
σ	standard deviation in activation energies, kJ mol^{-1}
β_i	ith root of equation 12b

REFERENCES

1. Yaverbaum, L.H., 'Fluidized Bed Combustion of Coal and Waste Materials', Noyes Data Corporation (1977).

2. Selle, S.J., Honea, F.I. and Sondreal, E.A., in 'New Fuels and Advances in Combustion Technology', Institute of Gas Technology, Chicago, 1979.

3. Jung, K. and Stanmore, B.R., Fuel, 1980, Vol. 59, p. 74.

4. Keey, R.B., in 'Advances in Drying', (Ed. A.S. Mujumdar), Hemisphere Publishing Corporation, Washington, 1980, Vol. I, p. 1.

5. Dayan, A., Int. J. Heat Mass Transfer, Vol. 25, 1982, p. 1469.

6. Agarwal, P.K., Genetti, W.E., Lee, Y.Y. and Prasad, S.N., to appear in Fuel.

7. Mori, A. and Araki, K., Intl. Chem. Eng., Vol. 16, 4, 1976, p. 734.

8. Crank, J. in 'Moving Boundary Problems in Heat Flow and Diffusion', (ed. Ockendon, J.R. and Hodgkins, W.R.), Clarendon Press, Oxford, 1975, p. 192.

9. Tao, L.N., Quarterly J. of Mech. and Appl. Math., Vol. 32, Pt. 2, 1979, p. 175.

10. Shamsundar, N. in 'Moving Boundary Problems', (ed. Wilson, D.G., Solomon, A.D. and Boggs, P.T.), Academic Press, New York, 1978, p. 165.

11. Anthony, D.B. and Howard, J.B., AIChE J., Vol. 22, 4, 1976, p. 625.

12. Gavalas, G.R., 'Coal Pyrolysis', Elsevier Scientific Publishing Co., New York, 1982.

13. Juntgen, H. and van Heek, K.H., Fuel Processing Technology, 2 (1979), p. 261.

14. Peters, W. and Bertling, H., Fuel, Vol. 44, 1965, p. 317.

15. Borghi, G., Sarofim, A.F. and Beer, J.M., paper presented AIChE 70th Annual Meeting, New York, November, 1977.

16. Mills, A.F., James, R.K. and Antoniuk, D., in 'Future Energy Production Systems', Vol. 2, (ed. Denton, J.C. and Afgan, N.H.), Washington, 1976, p. 537.

17. Essenhigh, R.H., J. Eng. Power, Vol. 85, 1963, p. 183.

18. LaNauze, R.D., Fuel, Vol. 61, 1982, p. 771.

19. Agarwal, P.K., Genetti, W.E. and Lee, Y.Y., (Submitted for publication).

20. Agarwal, P.K., Genetti, W.E. and Lee, Y.Y., to appear in Chem. Engg. Comm.

21. Jakob, M., 'Heat Transfer', John Wiley and Sons, New York, 1959.

22. Agarwal, P.K., Genetti, W.E., and Lee, Y.Y. (Submitted for publication).
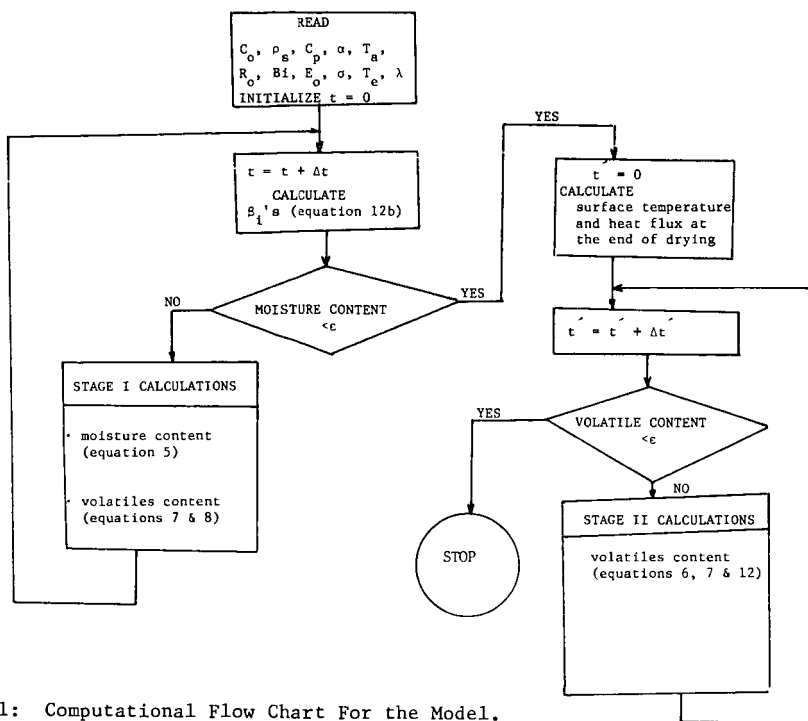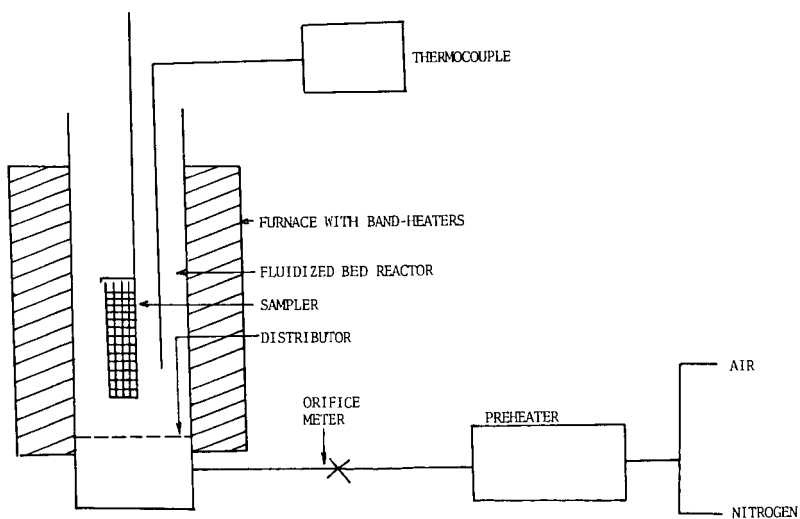
Figure 1: Computational Flow Chart For the Model.

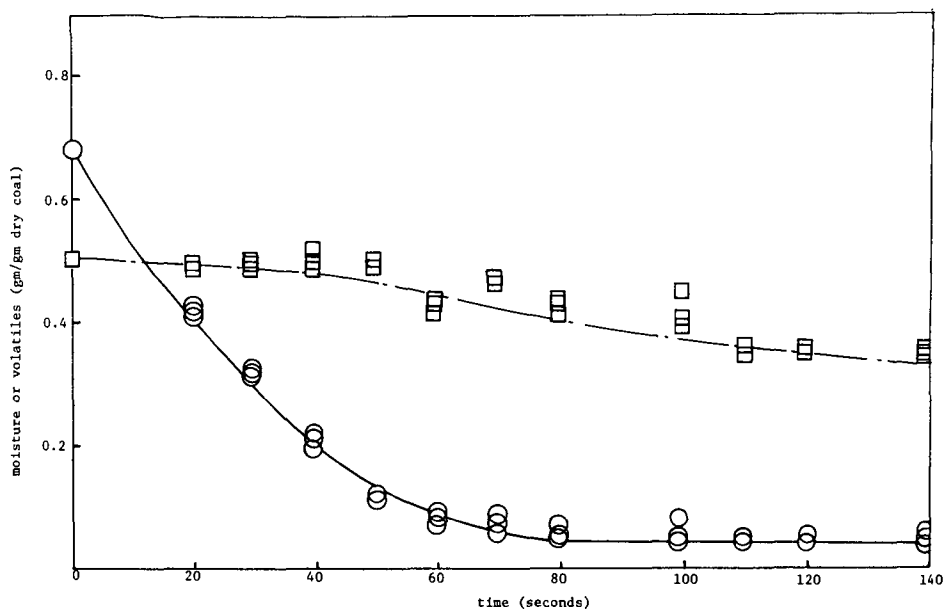Figure 2: Experimental Apparatus Schematic.

Figure 3: Experimental Data and Model Predictions for Drying (0, —) and
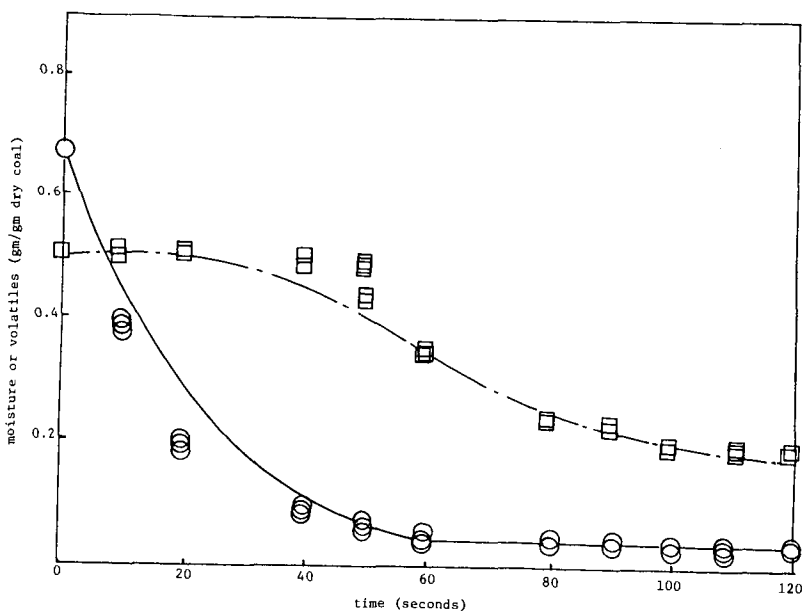Devolatilization (, — - —) at 613°K

Figure 4: Experimental Data and Model Predictions for Drying (0, —) and
Devolatilization (, — - —) at 713°K.